Unusual Photoluminescent Properties of the 3D Mixed-Lanthanide-Organic Frameworks Induced by Dimeric Structure: A Theoretical and Experimental Approach

Carime V. Rodrigues,[a] Leonis L. Luz,[b] José Diogo L. Dutra,[c] Severino A. Junior,[b] Oscar L. Malta,[b] Claudia C. Gatto,[a] Huayna C. Streit,[d] Ricardo O. Freire,[c] Claudia Wickleder,*[d] and Marcelo Oliveira Rodrigues*[a]*

[a] Instituto de Química, Campus Universitário Darcy Ribeiro, CEP 70904970, P.O.Box 4478, Brasilia-DF, Brazil.
[b] Departamento de Química Fundamental, UFPE, 50590-470, Recife - PE, Brazil.
[c] Pople Computational Chemistry Laboratory, Departamento de Química, Universidade Federal de Sergipe, 49100-000, São Cristóvão, Sergipe, Brazil.
[d] Inorganic Chemistry, Department of Science and Technology, University of Siegen. Adolf-Reichwein-Strasse 2, 57068 Siegen, Germany.

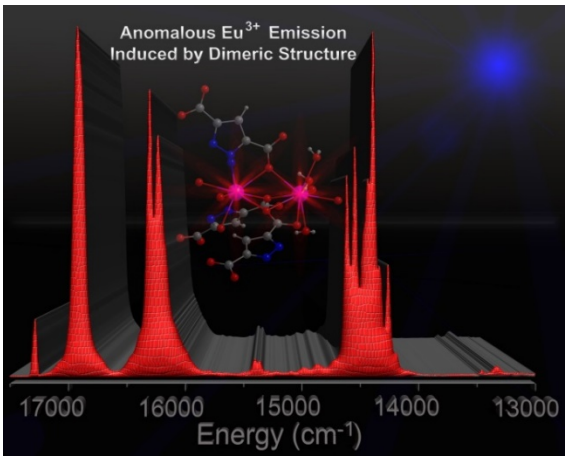

SUMMARY:

Experimental Section---------- II
Table 1S---------- III
Table 2S---------- IV
Figure 1S---------- V
Figure 2S---------- VI
Table 3S---------- VII
Table 4S---------- VII
Figure 3S---------- VIII
Figure 4S---------- VIII
Figure 5S---------- IX
Figure 6S---------- X
Figure 7S---------- XI
Figure 8S---------- XI

Experimental Section

A mixture of pyrazole-3,5-dicarboxylic acid, H_2PDC, (0.3 mmol), $LnCl_3.5H_2O$, (0.2 mmol, Ln = La^{3+}, Eu^{3+} and Tb^{3+} in appropriate ratios, 0.2/0/0 , 0.18/0.02/0, 0.18/0/0.02 and 0.18/0.01/0.01, herein designated as **(1)** to **(4)** respectively, and H_2O (*ca.* 12 mL) were hydrothermally treated in a 23 mL Teflon-lined stainless steel autoclave at 170ºC for 72h. The final materials were insoluble in water or common organic solvents, were obtained in an average yield of *ca.* 35% after washed with water, acetone and air-dried.

Photoluminescence spectra and lifetime measurements were collected using a FLUOROLOG3 ISA/Jobin-Yvon spectrofluorometer equipped with Hamamatsu R928P photomultiplier a SPEX 1934 D phosphorimeter, a 450 W Xe arc lamp and a pulsed 150W Xe-Hg lamp. All spectra were corrected for the spectral response of the monochromators and the detector corrected via correction spectra provided by the manufacturer. Additionally, the excitation spectra were correct for the spectral distribution of the lamp intensity from 240-600 nm using a photodiode as reference. Absolute Quantum Yield (QY) values were acquired by using the Fluorolog 3 spectrometer, with an additional Ulbricht sphere. Thermogravimetric and Differential Thermal Analysis (TGA/DTA) curves were performed using a Shimadzu Simultaneous TGA/DTA Analyzer DTG-60AH, in the 25-600 ºC temperature range, using an alumina crucible with *ca.* 8.0 mg of sample, under dynamic nitrogen atmosphere (50 $ml \cdot min^{-1}$) and with a heating rate of 10 $K \cdot min^{-1}$. The FT-IR spectra were recorded from KBr pellets (in the 400-4000 cm^{-1} spectral range) using a BRUKER IFS 66.

Table 1S. Crystal and structure refinement data for $[Ln_2(PDC)_3(H_2O)_4].2H_2O$.

Formula	$C_{15}\ H_{18}\ La_2N_6O_{18}$
Formula weight	848.17
Crystal system	Monoclinic
Space group	*Cc*
Temperature/K	296(2) K
Unit cell dimensions /Å	a = 15.815(2) Å
	b = 8.892(10) Å
	c = 18.430(2) Å
	γ = 98.393(10)°
Volume/Å^3	2564.15(5) Å^3
Z	4
D_c/g cm^{-3}	2.189
μ(Mo-Kα)/mm^{-1}	3.383
Crystal size/mm	0.238 x 0.172 x 0.138
θ range	2.23 to 30.63°
Index ranges	$-22 \le h \le 22$
	$-11 \le k \le 12$
	$-26 \le l \le 26$
Reflections collected	19493
Independent reflections	7448 (R_{int} = 0.0380)
Completeness to theta = 30.63°	99.9 %
Final *R* indices [I>2σ(I)][a,b]	*R1 = 0.0271*
	wR2 = 0.0538
Final *R* indices (all data)[a,b]	*R1 = 0.0292*
	wR2 = 0.0550
Largest diff. peak and hole	1.136 and
	-0.680 e.Å^{-3}
CCDC Deposition Number	948808

[a] $R1 = \sum \left| |F_o| - |F_c| \right| / \sum |F_o|$; [b] $wR2 = \sqrt{\sum \left[w\left(F_o^2 - F_c^2\right)^2 \right] / \sum \left[w\left(F_o^2\right)^2 \right]}$

Table 2S. Selected bond lengths (Å) and bond angles (°) for $[Ln_2(PDC)_3(H_2O)_4].2H_2O$.

La1-La2 = 4.067(3)	La1–O1–La2 = 101.25(10)
La1-O1 = 2.632(3)	La1–O9–La2 = 103.50(10)
La1-O3 = 2.466(3)	O1–La1–N1 = 60.77(10)
La1-O5 = 2.630(3)	O5–La1–N3 = 60.83(10)
La1-O8 = 2.461(3)	La1–O1–La2 = 101.25(10)
La1-O9 = 2.495(3)	La1–O9–La2 = 103.50(10)
La2-O5 = 2.569(3)	O1–La1–N1 = 60.77(10)
La2-O10 = 2.622(4)	O5–La1–N3 = 60.83(10)
La2-O13 = 2.559(4)	
La2-O14 = 2.619(4)	
La1-N1 = 2.651(4)	
La1-N3 = 2.670(4)	
La1-N6 = 2.684(4)	

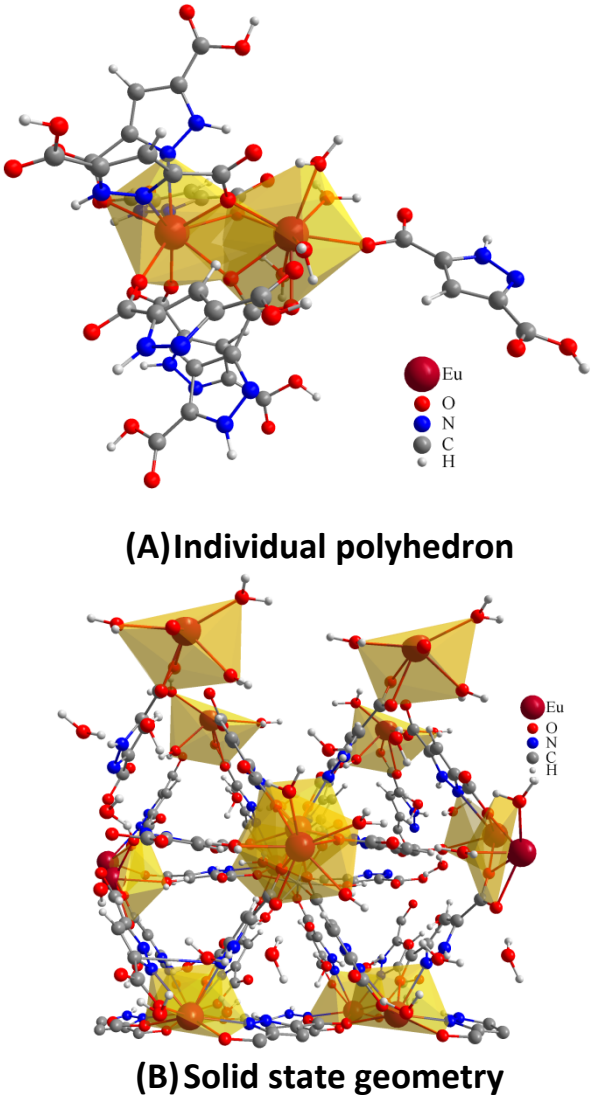

Figure 1S. Ground State solid geometry of the $[Eu_2(PDC)_3(H_2O)_4].4H_2O$ calculated using the Sparkle/PM3 model.

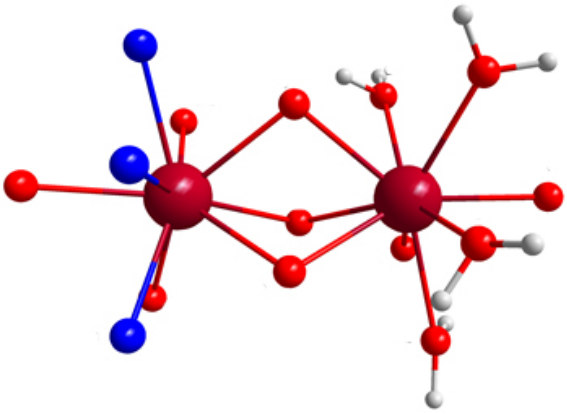

(A) Ligand atoms numbers

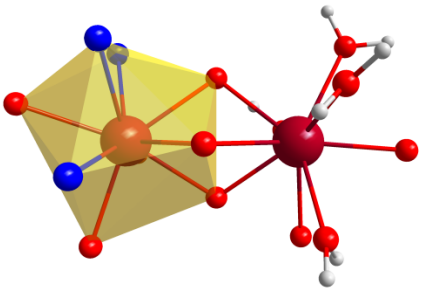

(B) Polyhedron 1

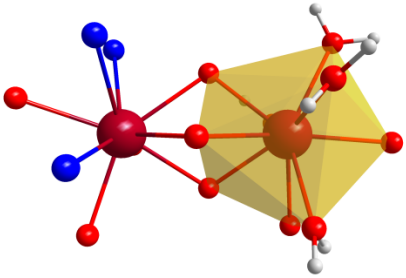

(C) Polyhedron 2

Figure 2S. Optimized geometries of the polyhedra.

Table 3S. Calculated values of intramolecular energy transfer and back-transfer rates for **(2)** system. The R_L value is the distance from the donor state located at the organic ligands and the Eu^{3+} ion nucleus.

(2)	Ligand State (cm^{-1})		4f – State (cm^{-1})	R_L (Å)	Transfer Rate (s^{-1})	Back-Transfer Rate (s^{-1})
Eu (1)	Singlet (36821.9)	→	$^5D_4$(27586)	3.87	4.86 x10^3	2.72 x 10^{-16}
	Triplet (27163.6)	→	$^5D_1$(19027)	5.92	1.11 x 10^8	1.41 x 10^{-9}
	Triplet (27163.6)	→	$^5D_0$(17293)	5.92	2.65 x 10^7	6.79 x 10^{-14}
Eu (2)	Singlet (41940.5)	→	$^5D_4$(27586)	6.08	4.59 x 10^{-2}	5.30 x 10^{-32}
	Triplet (18398.9)	→	$^5D_1$(19027)	6.18	6.67 x 10^9	1.68 x 10^{11}
	Triplet (18398.9)	→	$^5D_0$(17293)	6.18	1.22 x 10^{10}	6.19 x 10^7

Table 4S – Numerical estimative of the ET process.

	λ= 2	λ= 4	λ= 6
$\langle l \Vert C^{\lambda} \Vert l \rangle$	-1.366	1.128	-1.27
$\langle r^{\lambda} \rangle$ (Eu^{3+})	0.9175	2.0200	9.0390
$\langle r^{\lambda} \rangle$ (Tb^{3+})	0.8220	1.6510	6.8520
σ_{λ} (Eu^{3+})	0.502	0.0190	-0.0308
σ_{λ} (Tb^{3+})	0.486	0.0193	-0.0300

σ_1 (Tb^{3+}) = σ_1 (Eu^{3+}) = 0.900

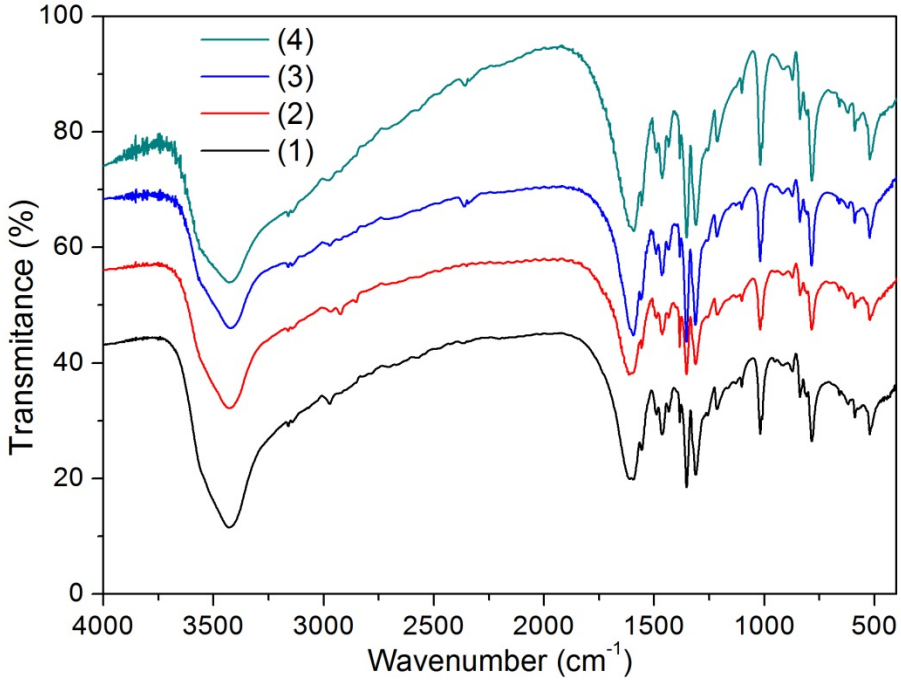

Figure 3S. IR spectra. **(1)**: Black solid line; **(2)**: Red solid line; **(3)**: Blue solid line; **(4):** Dark cyan solid line.

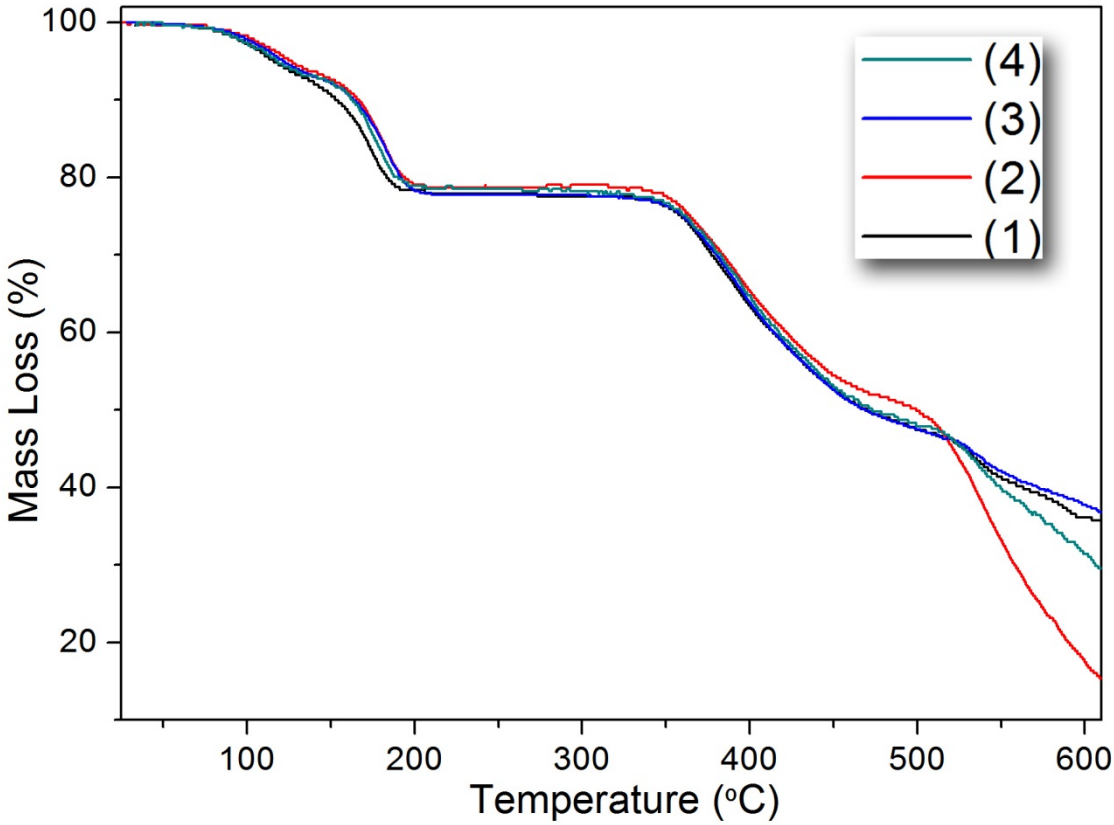

Figure 4S. TGA curves. **(1)**: Black solid line; **(2)**: Red solid line; **(3)**: Blue solid line; (4): Dark cyan solid line.

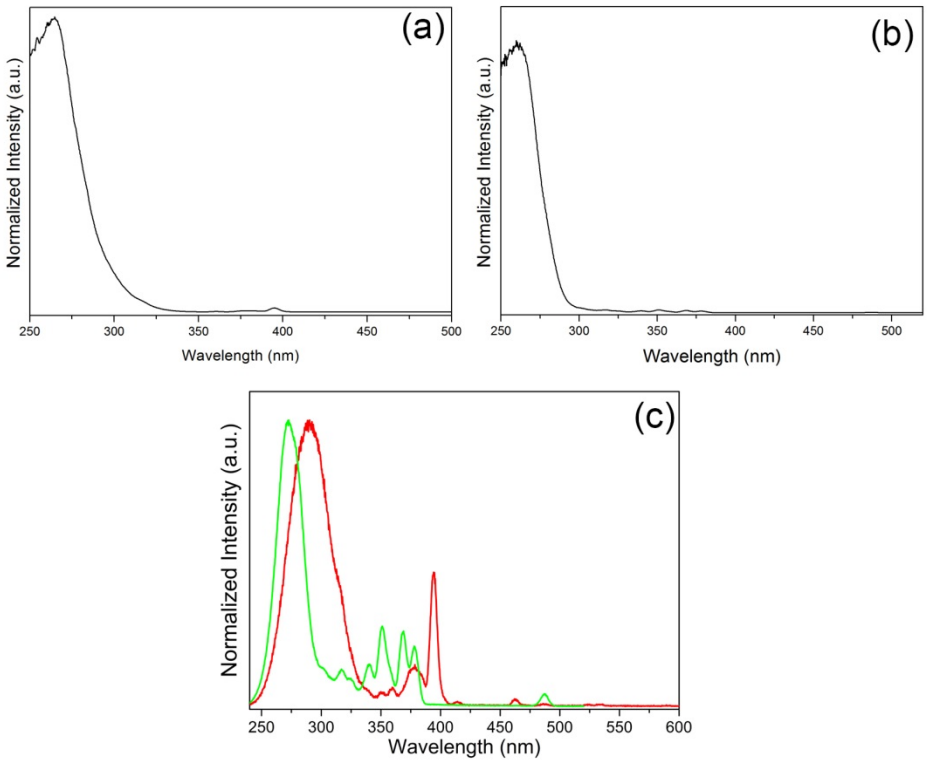

Figure 5S. Excitation spectra of **(4)**. (a) and (b) Corrected spectra using a photodiode as reference by monitoring the Eu^{3+} and Tb^{3+} emissions at 591 and 543 nm, respectively; (c) Excitation spectrum corrected only for the spectral response of the monochromators and the detector by monitoring the Eu^{3+} (red solid line) and Tb^{3+} (green solid line) emissions.

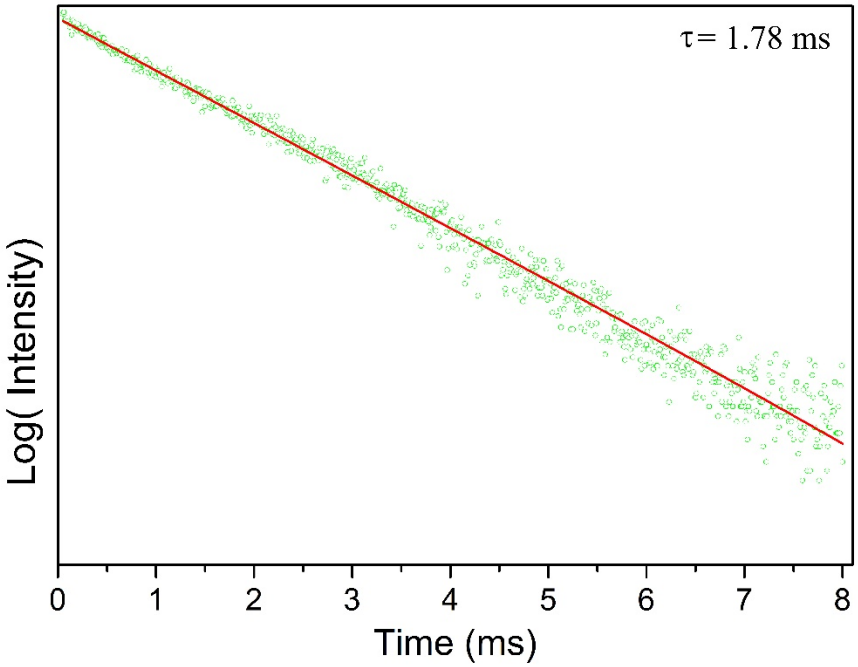

Figure 6S. Normalized decay curve of **(3)** at room temperature, upon excitation at 270 nm and by monitoring the Tb $^5D_4 \rightarrow {}^7F_5$ transition at *ca.* 543 nm. Red solid line corresponds to the best fit.

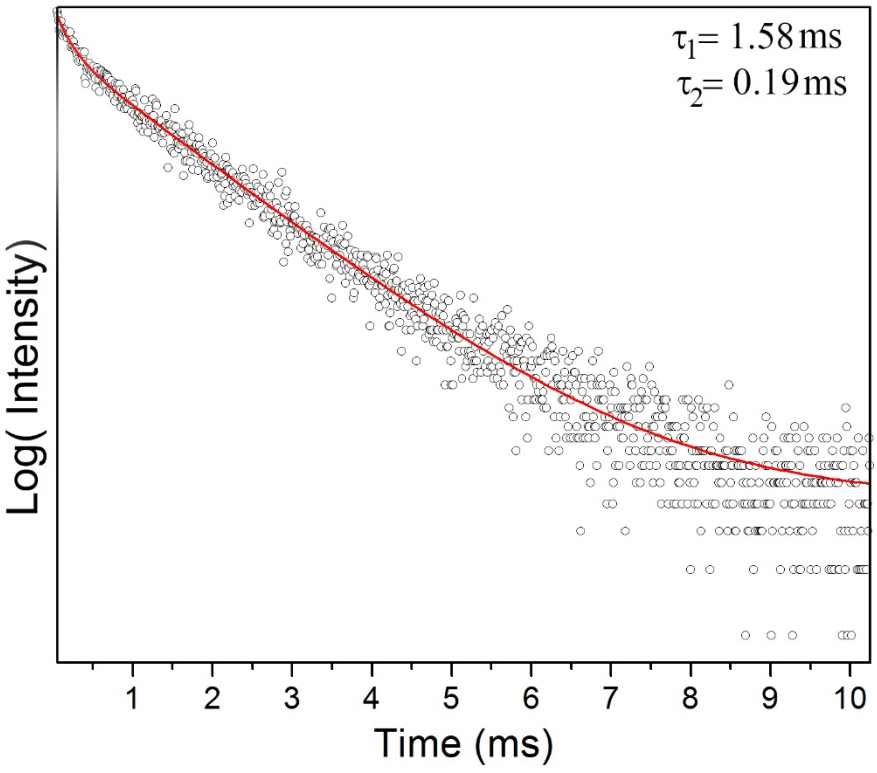

Figure 7S. Normalized decay curve of **(4)** at room temperature, upon excitation at 270 nm and by monitoring the Eu $^5D_0 \rightarrow {}^7F_1$transition at *ca.* 591 nm. Red solid line corresponds to the best fit.

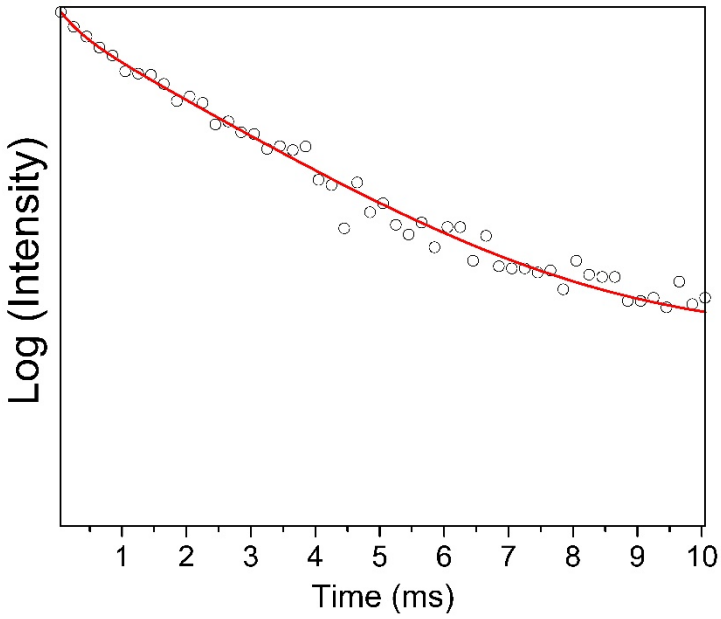

Figure 8S. Normalized decay curve of **(4)** at room temperature, upon excitation at 270 nm and by monitoring the Tb $^5D_4 \rightarrow {}^7F_5$ transition at *ca.* 543 nm. Red solid line corresponds to the best fit.